Chapter 6: Direct Electrochemistry of Endonuclease III in the Presence and Absence of DNA

Adapted from: Gorodetsky, A. A., Boal, A. K., Barton, J. K. (2006) *J. Am. Chem. Soc.* *128*, 12082–12083.

Endonuclease III was expressed and purified by Amie Boal.

ABSTRACT

The electrochemistry of the base excision repair enzyme Endonuclease III (Endo III) in the presence and absence of DNA has been examined on highly oriented pyrolytic graphite (HOPG). At the surface modified with pyrenated DNA, a reversible signal is observed at 20 mV versus NHE for the $[4Fe\text{-}4S]^{3+/2+}$ couple of Endo III, similar to Au. Without DNA modification, oxidative and reductive signals for the [4Fe-4S] cluster of Endo III are found on bare HOPG, allowing a direct comparison between DNA-bound and free redox potentials. These data indicate a shift of approximately -200 mV in the 3+/2+ couple upon binding of Endo III to DNA. This potential shift reflects a difference in affinity for DNA of more than 3 orders of magnitude between the oxidized 3+ and reduced 2+ protein and provides quantitative support for our model utilizing DNA-mediated charge transport to redistribute base excision repair enzymes in the vicinity of damaged DNA.

6.1 Introduction

In vivo, DNA is constantly being assaulted and damaged (1, 2). To protect the integrity of the genome, an impressive detection and repair network has evolved. However, macromolecular crowding, low repair enzyme copy number, and small structural differences in DNA lesions are dramatic challenges faced by the cell in damage detection. Consequently, the mechanisms by which DNA binding proteins can locate their substrates in rapid fashion are not well understood.

Base excision repair (BER) is one component of the DNA detection and repair machinery (3). In BER, glycosylase enzymes must scan a large and topologically complex genome for chemically modified bases and catalyze their excision. While much is known about the catalysis and substrate discrimination steps, very little is known about the daunting initial search of the genome these enzymes must undertake. Since glycosylase enzymes move processively along DNA, processive searches along DNA may represent one component of detection (4–7), but the *in vivo* relevance of this mechanism has been brought into question (8–10). Therefore, we have proposed DNA-mediated charge transport as the first step in damage detection since it provides a means to redistribute base excision repair proteins in the vicinity of damage rapidly and efficiently (11–14).

Endonuclease III and MutY are glycosylase enzymes which repair damaged pyrimidines and have been extensively characterized from a structural and biophysical perspective (3, 15–32). Crystal structures of these enzymes indicate that they both contain an iron-sulfur cluster with the C-X_6-C-X_2-C-X_5-C motif in close proximity to the DNA

backbone (15–18). EPR experiments demonstrated that the cluster is in its $[4Fe\text{-}4S]^{2+}$ form when isolated from the cell, but the protein cannot be reduced within a physiologically relevant window nor oxidized by ferricyanide without degradation (20, 21). Although these experiments indicated a structural role for the cluster, they were conducted in the absence of DNA. Notably, the [4Fe-4S] cluster was later found not necessary for protein folding or stability in MutY; this argued against a simple structural role, especially because the cluster was crucial for DNA binding and *in vivo* glycosylase activity (30–32). Subsequently, we demonstrated for both Endo III and MutY that the cluster is activated toward oxidation upon enzyme binding to DNA, and this DNA-dependent redox activity promotes charge transport through DNA (11–14).

DNA-modified electrodes have proven particularly useful for probing the redox properties of BER enzymes in their DNA-bound, biologically relevant forms (11, 12, 33). Electrochemistry of MutY and Endo III on DNA-modified gold electrodes shows a redox potential of ~ 60 mV and ~ 90 mV versus NHE respectively for the $[4Fe\text{-}4S]^{3+/2+}$ couple. Importantly, these signals were not observed at surfaces backfilled with mercaptohexanol but lacking DNA (11). Furthermore, weak signals were found on surfaces modified with DNA duplexes containing an abasic site, demonstrating that the observed redox processes for the proteins are DNA-mediated (11). Overall, DNA binding appears to shift the potential of Endo III and MutY, so that the proteins bound to DNA are more similar to high-potential iron proteins than ferredoxins (34–36).

We have recently explored the electrochemical properties of highly oriented pyrolytic graphite modified with pyrenated DNA as an attractive alternative to gold (37). The DNA monolayers formed on HOPG have been extensively characterized via

electrochemistry, AFM, and radioactive labeling and are quite similar to thiolated DNA films on gold (38–41). However, the accessible potential window is significantly larger on graphite, and moreover, graphite electrodes are particularly well suited for protein electrochemistry (42–49). Since previous work had shown that, without DNA binding, the $[4Fe\text{-}4S]^{2+}$ cluster is not readily oxidized or reduced within a physiological range of potentials (20, 21), we compared the electrochemical properties of Endo III in the presence and absence of DNA (Figure 6.1). Here, we directly demonstrate the shift in potential associated with DNA binding using HOPG electrodes.

6.2 Experimental Section

6.2.1 Materials

All reagents for DNA synthesis were purchased from Glen Research. All other reagents used in DNA and electrode preparation/processing were purchased from Sigma in the highest purity available and used as received. SPI-1 grade HOPG was purchased from SPI, Inc., and pyrolytic graphite was purchased from Union Carbide, Inc. Buffers were prepared with Milli-Q water and filtered with a 0.2 μm filter.

6.2.2 General DNA Synthesis and Preparation

Oligonucleotides were prepared using standard phosphoramidite chemistry on an ABI 392 DNA Synthesizer. DNA was purified by HPLC on a reverse phase C18 column with acetonitrile and ammonium acetate as the eluents. Unless otherwise noted, all oligonucleotides were cleaved from the resin with concentrated ammonium hydroxide

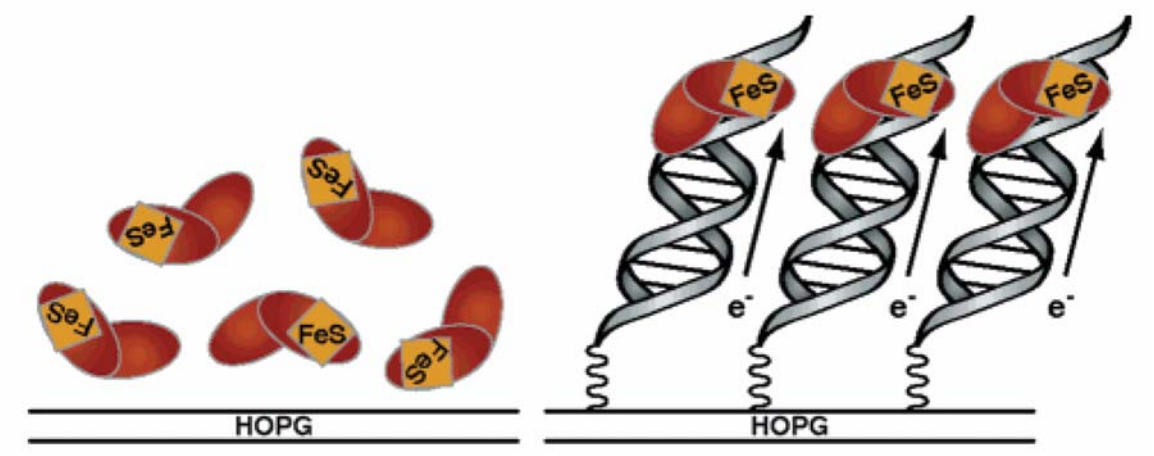

Figure 6.1: Schematic representation of electrochemistry for Endo III on HOPG with and without modification with DNA

(NH_4OH) prior to purification. The desired products were characterized by UV-visible spectroscopy and MALDI-TOF mass spectrometry.

As previously described (37), pyrene-terminated oligonucleotides with a long pyrene-to-DNA linker were prepared by solid-phase synthesis on a CPG resin with an unprotected hydroxyl group at the 5' terminus. The 5'-OH was treated with a 120 mg/mL solution of carbonyldiimidazole in dioxane for 90 minutes followed by an 80 mg/mL solution of 1,6-diaminohexane. The free amine was then treated with 1-pyrenebutyric acid *N*-hydroxysuccinimidyl ester, leaving a pyrene moiety at the 5' terminus.

Pyrene-terminated oligonucleotides with a short pyrene-to-DNA linker were also prepared as previously described (37). In brief, 500 mg of *N*,*N*-diisopropylethylamine was added to 5 mL of a 20 mg/mL solution of 1-pyrenebutanol in acetonitrile under an inert argon atmosphere. While the reaction mixture was gently stirred, 90 mg of *N*,*N*-diisopropylphosphoramidochloridite was added dropwise. The reaction progress was monitored by TLC before the reaction mixture was moved to an extraction funnel and washed twice with 5% (by volume) $NaHCO_3$ and 3 M NaCl. The organic layer was collected, dried with Na_2SO_4, and rotovapped to a yellow oil. The phosphoramidite was dissolved in 1 mL of acetonitrile and used immediately. On the synthesizer, the free hydroxyl at the 5' terminus of the oligonucleotide was condensed with a 2-cyanoethyl *N*,*N*-diisopropylphosphoramidite of 1-pyrenebutanol.

Pyrene-modified single-strand DNA was hybridized with its complement by heating equimolar amounts of each strand (typically 100 µM) in pH 7.1 buffer containing 5 mM P_i and 50 mM NaCl to 90 ºC, followed by cooling to ambient temperature. Since

single-stranded DNA can adsorb to graphite, great care was taken during quantification of DNA to ensure that equimolar amounts of each strand were annealed to form duplexes.

6.2.3 Expression and Purification of Endonuclease III

Eight separate batches of protein were utilized for the electrochemical experiments described. Endo III was expressed and purified according to previously reported procedures (50, 51). MutY was 1) generously donated by the David Lab (UC-Davis) and 2) purchased from Trevigen, Inc. and dialyzed against Endo III storage buffer.

6.2.4 Preparation of Bare and DNA-Modified HOPG Electrodes

DNA-modified surfaces were prepared on custom-built highly oriented pyrolytic graphite electrodes as previously described (37, 52). Briefly, the HOPG surface was cleaned with 3-M scotch tape before each experiment and mounted in the electrode housing. Duplex DNA containing a pyrene moiety was deposited onto the HOPG surface in pH 7.1 buffer containing 5 mM P_i 50 mM NaCl in the absence of Mg^{2+} to ensure a loosely packed film. DNA films were then allowed to form in a humidified chamber over a period of 24–48 hours. To ensure experimental consistency, bare electrodes were prepared in an identical fashion with the DNA omitted in the steps above.

When necessary, the bare or DNA-modified graphite surfaces were backfilled with short chain alkanes (53). The surface was rinsed thoroughly with Endo III storage buffer (pH= 7.5, 20 mM NaP_i, 100 mM NaCl, 1 mM EDTA) before being backfilled for ~ 1–2 hours with a 5% by volume octane solution in a 1:1 Endo III storage buffer/glycerol solution. Large percentages of glycerol or small percentages of ethanol were used to improve the poor solubility of alkanes in the Endo III storage buffer. The electrodes were then thoroughly cleaned with multiple rinses of storage buffer.

6.2.5 Preparation of Didodecyldimethylammonium-Modified Pyrolytic Graphite Electrodes

Didodecyldimethylammonium bromide (DDAB) modified pyrolytic graphite (PG) surfaces were prepared as previously described (47–49). Briefly, electrodes were made from the basal plane of pyrolytic graphite and pretreated by abrasion with sandpaper, brief sonication in deionized H_2O, and drying with a heat gun. Didodecyldimethylammonium films were applied by incubating the surface in a saturated DDAB solution in a humidified environment overnight.

6.2.6 Electrochemical Measurements on HOPG

Prior to incubation with protein, bare or DNA-modified HOPG electrodes were cooled to 4 ºC. Although this was not done in all experiments, cooling of the electrodes was found to dramatically improve protein stability. Bare or DNA modified electrodes were incubated with protein for ~ 1–4 hours prior to electrochemical measurements. Blank electrodes were treated in an identical fashion with the protein omitted. Cyclic and square wave voltammetry experiments were subsequently recorded on either a CH Instruments electrochemical analyzer (Austin, TX) or a Bioanalytical Systems CV-50W potentiostat using the inverted drop cell configuration. All measurements reported for the working electrode were taken versus a platinum (Pt) auxiliary and a silver/silver chloride (Ag/AgCl) reference. The Ag/AgCl reference was frequently standardized versus SCE. Unless otherwise noted, experiments were performed at ambient temperature in Endo III storage buffer.

6.2.7 Electrochemical Measurements on Pyrolytic Graphite

The electrodes were incubated with a 50 µM Endo III solution for ~ 6 hours in the presence or absence of an excess of DNA at 4 º C. The protein-modified electrodes were rinsed thoroughly prior to electrochemistry experiments. Cyclic voltammetry experiments were subsequently recorded on either a CH Instruments electrochemical analyzer (Austin, TX) or a Bioanalytical Systems CV-50W potentiostat. Experiments were performed at ambient temperature in pH 8.0 buffer containing 20 mM KP_i and 100 mM KCl under an argon atmosphere. A custom-built three-compartment electrochemical cell was used for all experiments with a Pt auxiliary electrode, a PG working electrode, and a saturated calomel (SCE) reference electrode.

6.3 Results

6.3.1 Electrochemistry of Free and DNA-Bound Endo III on HOPG

Figure 6.2 shows cyclic voltammetry (CV) and square wave voltammetry (SWV) of Endo III on HOPG with and without DNA modification. For the DNA-modified electrode, a quasi-reversible redox couple is observed with a midpoint potential of 20 ± 10 mV versus NHE. Backfilling the DNA electrode with octane has no effect on this signal, while backfilling HOPG without DNA leads to the loss of any protein signal (Figure 6.3).

To establish that this signal is DNA-mediated, we also examined an electrode modified with DNA featuring an abasic site prepared under identical conditions;

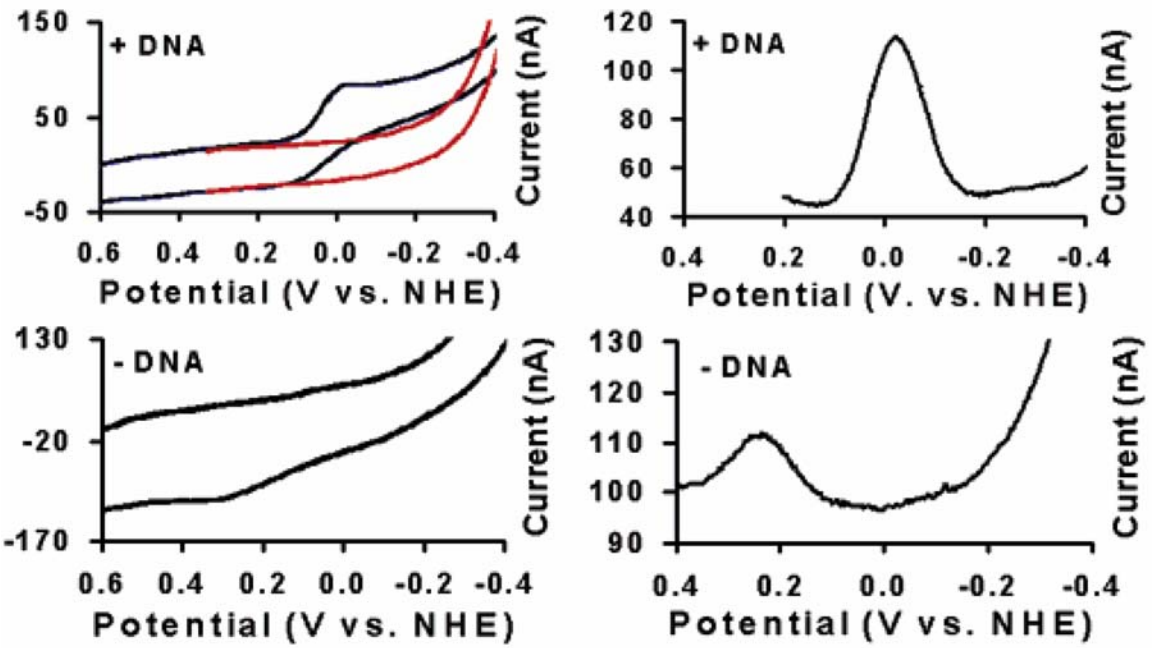

Figure 6.2: CV (left, 50 mV/s scan rate) and SWV (right, 15 Hz) of 50 µM Endo III in 20 mM Na phosphate, 100 mM NaCl, 1 mM EDTA, 20% glycerol, pH 7.5 buffer. The top two panels show electrochemistry of Endo III at a HOPG electrode modified with the sequence pyrene-$(CH_2)_4$-Pi-5'-AG*T* ACA GTC ATC GCG-3' plus complement. Cyclic voltammetry of a HOPG electrode modified with DNA featuring an abasic site is in red (top left), where the abasic position corresponds to the complement of the italicized base. The bottom two panels show electrochemistry of Endo III on bare HOPG.

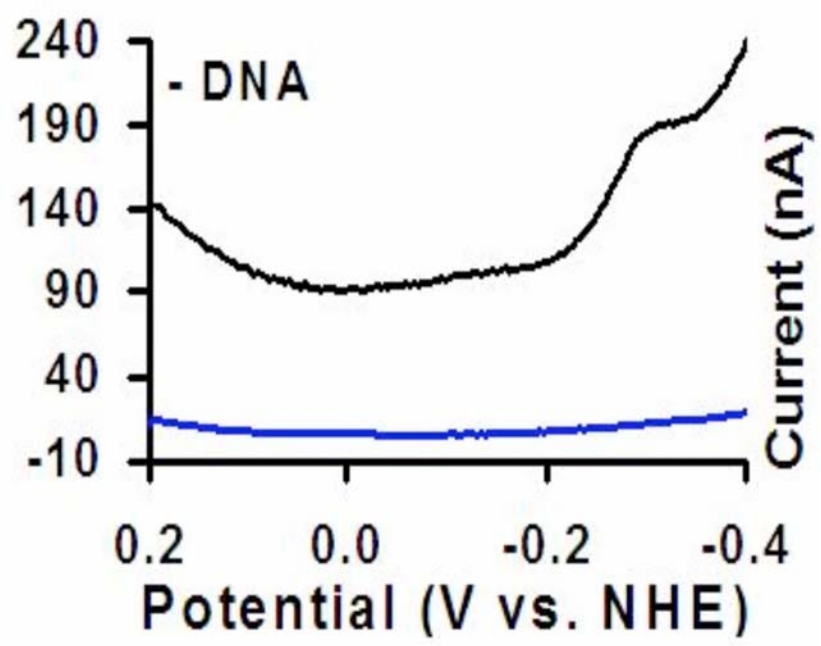

Figure 6.3: SWV (15 Hz) of 50 µM Endo III in 20 mM Na phosphate, 100 mM NaCl, 1 mM EDTA, 20% glycerol, pH 7.5 buffer showing the 2+/1+ couple. An electrode backfilled with octane prior to incubation with protein is shown in blue. The two electrodes have been normalized by their geometric areas for clarity.

DNA-mediated charge transport has been shown to be inhibited by the abasic site owing to the disruption in base stacking (11, 12). As seen in Figure 6.2, a complete loss of signal for Endo III is observed at the electrode modified with DNA containing an abasic site. Thus the DNA does not serve to locally concentrate the protein on the graphite surface; the duplex with an abasic site would serve a similar function. Instead it is the *DNA-bound* protein that is probed electrochemically on HOPG in a DNA-mediated reaction, as long as the DNA duplex is well stacked.

Note that at the DNA-modified surface, we observe only one redox signal, with no other peaks evident in the range of 600 to -400 mV versus NHE. This signal is not observed for a DNA-modified electrodes in Endo III dialysis buffer (Figure 6.4). The only couple we observe features a cathodic peak at -30 ± 30 mV versus NHE whose shape and magnitude indicate slow diffusive kinetics, as found for MutY (11, 12). Indeed, in all respects, this couple resembles that found for Endo III at a DNA-modified Au surface (11, 12) and is assigned to the $[4Fe\text{-}4S]^{3+/2+}$ couple. EPR experiments in solution on DNA- bound MutY reveal *g* values characteristic of a 3+ cluster and support this assignment (13, 14).

Significantly, on HOPG versus Au, we may explore the electrochemistry of Endo III at a larger range of applied biases (37), and thus we may directly compare the electrochemistry of Endo III in the presence and absence of DNA. Oxidative scans of Endo III on bare HOPG reveal an irreversible anodic peak at 250 ± 30 mV versus NHE and no couple either at 20 mV as with DNA (Figure 6.2) or in Endo III dialysis buffer (Figure 6.4). However, we do observe a quasi-reversible wave at higher protein concentrations (Figure 6.5). Successive positive scans lead to new broad, irregular signals

A.

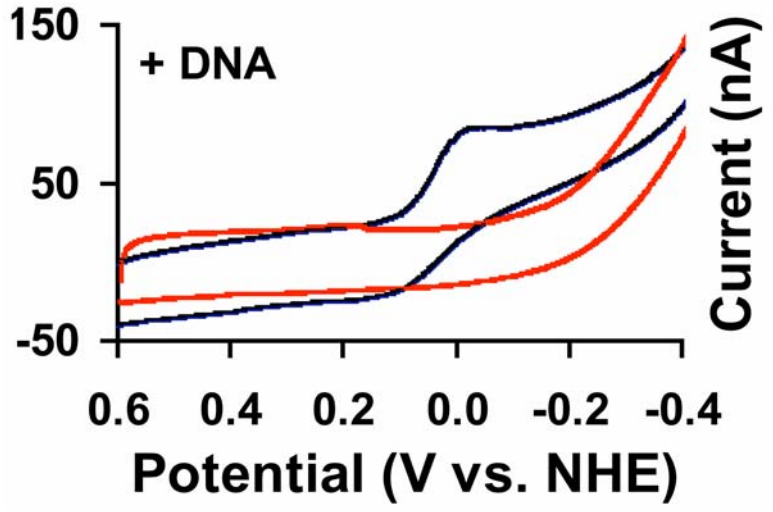

B.

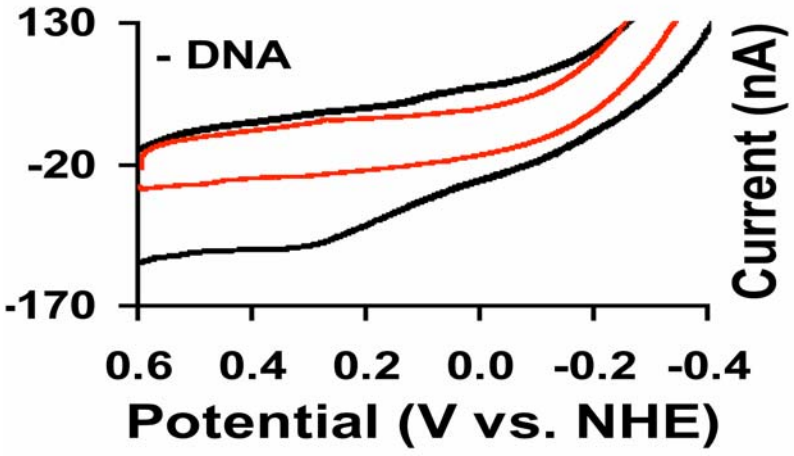

Figure 6.4: CV (left, 50 mV/s scan rate) and SWV (right, 15 Hz) of 50 µM Endo III in 20 mM Na phosphate, 100 mM NaCl, 1 mM EDTA, 20% glycerol, pH 7.5 buffer. The top panel shows electrochemistry of Endo III at a HOPG electrode modified with the sequence pyrene-$(CH_2)_4$-Pi-5'-AG*T* ACA GTC ATC GCG-3' plus complement (A). The bottom panel shows electrochemistry of Endo III at bare HOPG electrode (B). Voltammetry of the protein dialysis buffer in the absence of protein is shown in red for comparison.

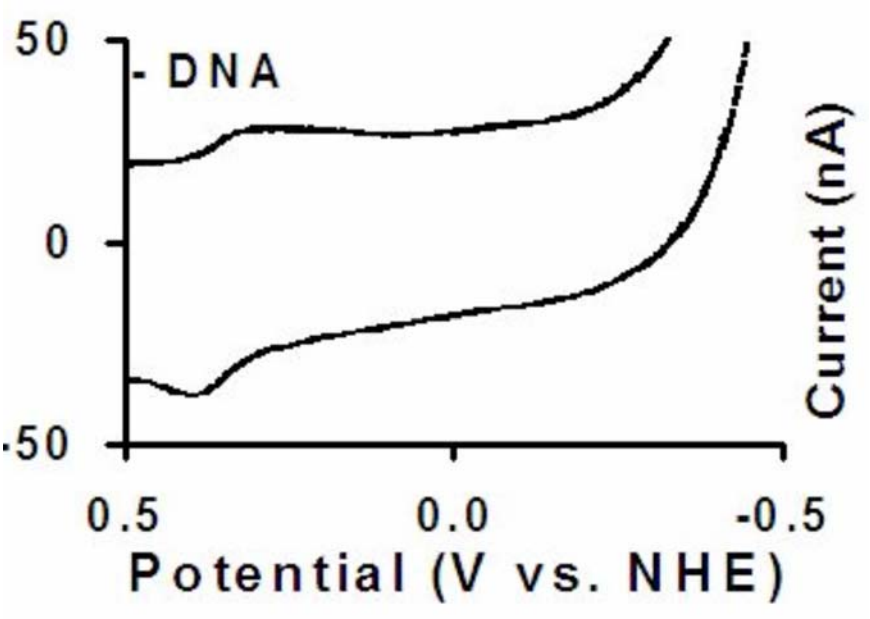

Figure 6.5: CV (50 mV/s scan rate) of 200 µM Endo III in 20 mM Na phosphate, 100 mM NaCl, 1 mM EDTA, 50% glycerol, pH 7.5 buffer on bare HOPG showing the 3+/2+ couple. Note that both cathodic and anodic peaks are observed here.

at approximately -80 and -710 mV versus NHE; additionally, the yellow color of the protein solution is lost. These results are fully consistent with oxidative decomposition of the cluster in Endo III without DNA and similar peaks are found with $FeCl_3$ controls (Figure 6.6). Indeed, these redox signals are commonly associated with ferredoxin [3Fe-4S] clusters (34, 35, 54).

It is noteworthy that on bare HOPG, we observe also the 2+/1+ couple of the [4Fe-4S] cluster during reductive scans with a cathodic peak at approximately -300 ± 80 mV versus NHE (Figure 6.3 and Figure 6.7). The peak is near the edge of our potential window, and this redox signal also contains a small oxidative wave at slow scan rates (Figure 6.7). In our experiments, the potential difference between 3+/2+ and 2+/1+ couples is somewhat smaller than expected (20, 21).

6.3.2 Electrochemistry of Free and DNA-Bound Endo III on Pyrolytic Graphite

Due to the frequently observed instability of Endo III on bare HOPG, the electrochemistry of Endo III was also investigated at DDAB modified pyrolytic graphite electrodes. Biomembrane-like films are commonly utilized in protein electrochemistry experiments (47–49). They are formed via the incubation of a graphite electrode with surfactants bearing a polar head group and a long, non-polar tail consisting of hydrocarbon chain. Such films possess the dual advantage of preventing adsorptive denaturation of proteins at the electrode surface and orienting the proteins for efficient electron transfer (47–49).

The electrochemistry of DDAB electrodes modified with Endo III in the presence and absence of DNA is shown in Figure 6.8. In the absence of DNA, two weak and irreversible signals are observed with cathodic waves at -180 mV and -370 mV versus

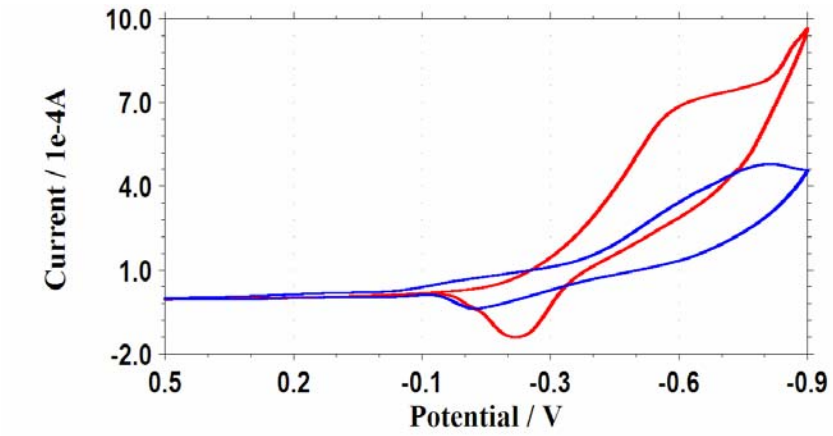

Figure 6.6: Typical CV (100 mV/s scan rate) of $FeCl_3$ on bare HOPG in 20 mM Na phosphate, 100 mM NaCl, 1 mM EDTA, 50% glycerol, pH 7.5 buffer. The voltammetry of free iron was recorded in the absence (blue) and presence (red) of thiol. The potential and reversibility of the free iron peak were both found to vary depending on the identity of the added alkanethiol (mercaptohexanol in this case).

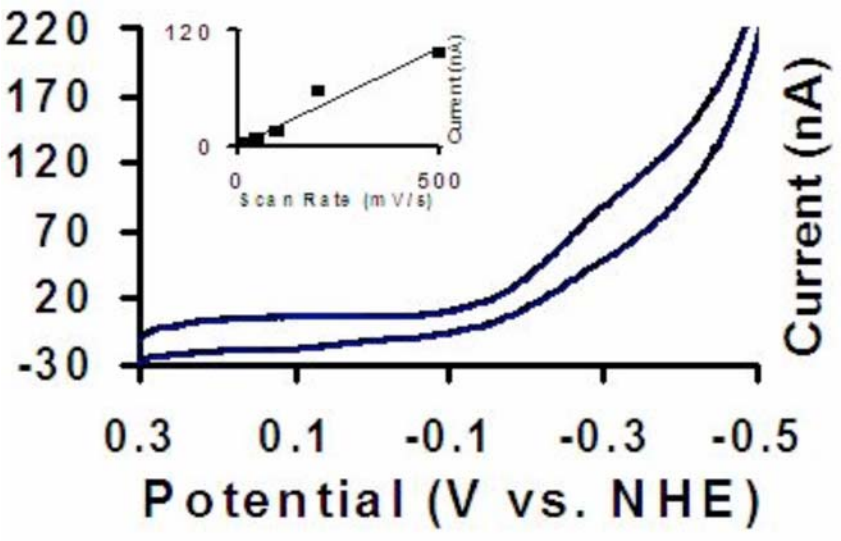

Figure 6.7: CV (20 mV/s scan rate) of 50 µM Endo III in 20 mM Na phosphate, 100 mM NaCl, 1 mM EDTA, 20% glycerol, pH 7.5 buffer on bare HOPG showing the 2+/1+ couple. A plot of peak current as a function of scan rate is inset.

A.

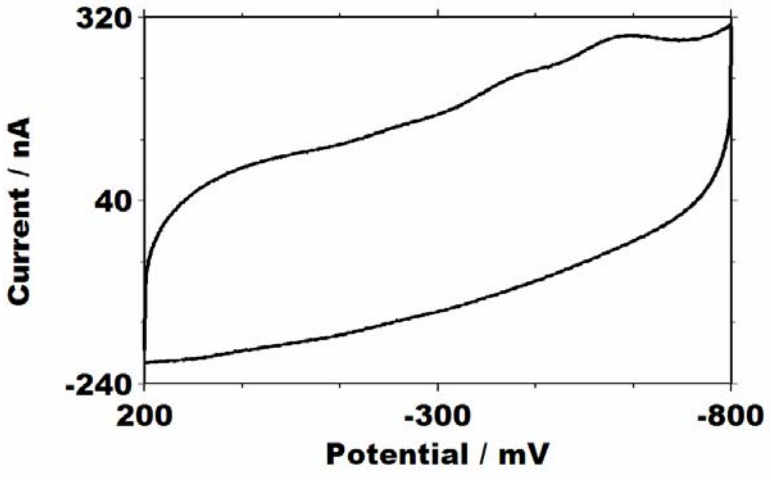

B.

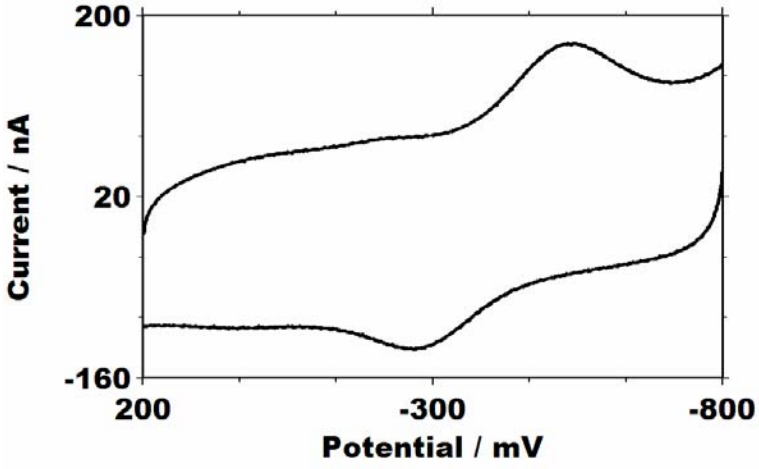

Figure 6.8: CV (20 mV/s scan rate) of Endo III in 20 mM K phosphate, 100 mM KCl, pH 8 buffer on a DDAB modified pyrolytic graphite. An electrode incubated with DNA bound Endo III is shown on the top panel (A), and an electrode modified with free Endo III is shown on the bottom panel. (B).

NHE, which can be assigned to the 2+/3+ and 2+/1+ couples, respectively. In the presence of DNA, Endo III is dramatically stabilized, and a single, large, and reversible redox couple is observed with a cathodic wave at -290 mV versus NHE, which can be assigned to its 2+/3+ couple. It is noteworthy that the potentials for free and DNA-bound Endo III in DDAB are different from the ones found on gold or graphite, which may indicate that Endo III does not maintain its native conformation in the positively charged, DDAB surfactant films. However, these experiments do provide support for the dramatically different electrochemical properties of Endo III observed in the presence and absence of DNA.

6.4 Implications and Discussion

Figure 6.9 summarizes the potentials we have observed for Endo III on HOPG over several trials. Although SWV gives a shift of 280 mV between the cathodic DNA-bound potential and the anodic potential on bare HOPG, the shift in midpoint potentials should be slightly smaller. Given the lack of reversibility and the supporting results obtained for Endo III in DDAB films on pyrolytic graphite, we can provide a lower estimate of ~ 200 mV for the change in redox potential by the 3+/2+ couple upon DNA binding; the corresponding change in the 2+/1+ couple cannot be easily determined.

The observed shift is understandable based upon the sensitivity of [4Fe-4S] cluster potentials to their environment (34–36). DNA binding clearly stabilizes the oxidized 3+ form of the cluster, whereas without DNA, it is $[4Fe\text{-}4S]^{2+}$ that is more stable. Crystal structures of Endo III with and without DNA reveal that the cluster is located

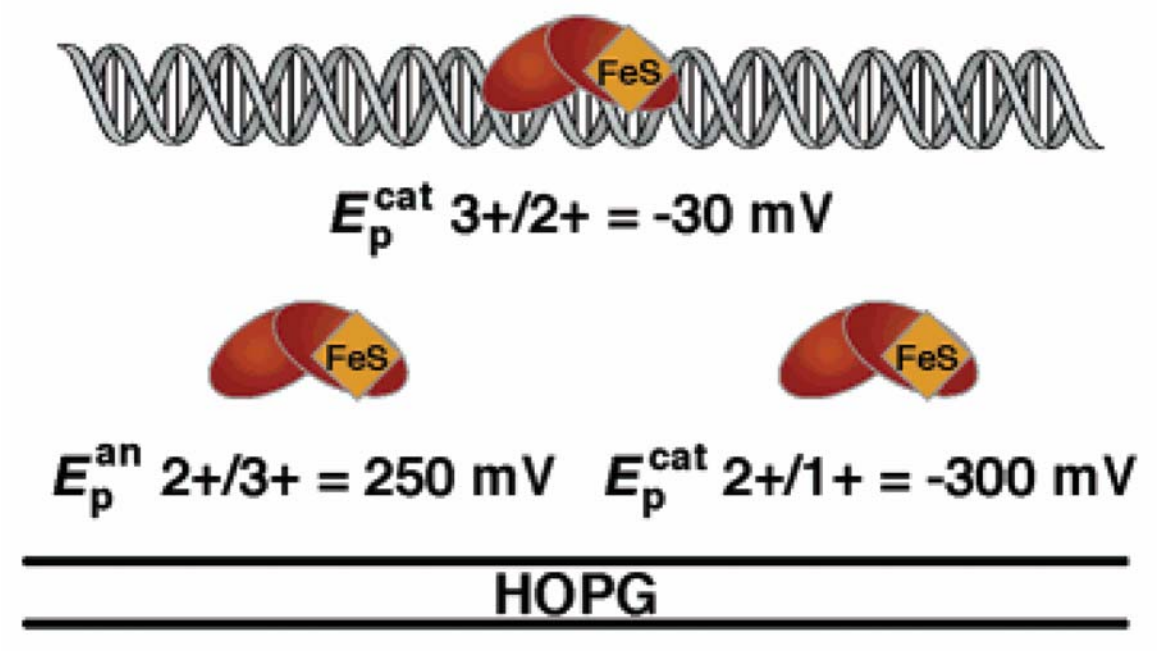

Figure 6.9: Illustration of the potentials versus NHE of the couples of Endo III in the presence and absence of DNA. These values are based upon SWV on HOPG and are averages of at least four trials each.

near amino acid residues that contact DNA (15–17). DNA binding takes the cluster to a more hydrophobic environment compared to the exposed and polar environment in the absence of DNA. Importantly, the resultant shift in potential is not associated with significant conformational changes in the protein; the structures of the bound and free proteins are remarkably similar. Instead, then, the ~ 200 mV shift in potential must correspond to a decrease in DNA binding affinity of more than 3 orders of magnitude between the 2+ and 3+ forms of the cluster.

While previous evidence qualitatively indicated a lessened DNA binding affinity for the reduced protein (12), these data provide a more quantitative estimate. In the context of our model of DNA-mediated signaling for damage detection, it is this difference in DNA binding affinity for the reduced versus oxidized state that leads to the dissociation of protein from the DNA upon reduction. This allows for the effective redistribution of BER proteins onto sites near damage, perhaps through long range electron transfer to other redox-active, DNA-binding proteins (13, 14).

We have, therefore, now identified the electrochemistry of Endo III both with and without DNA on HOPG electrodes. DNA binding is seen to promote a shift in redox potential, activating the protein toward oxidation; subsequent reduction of the cluster to the 2+ form leads to dissociation from the duplex. These results provide strong support for the detection strategy we have proposed for BER enzymes. Furthermore, these data underscore the importance of the outer sphere environment in regulating potentials of [4Fe-4S] proteins (34–36, 42–45), as well as the utility of DNA-modified electrodes in probing the redox characteristics of proteins that bind to DNA.

REFERENCES

(1) Friedberg, E. C., Walker, G. C., Siede, W. (1995) *DNA Repair and Mutagenesis*, ASM Press, Washington, D. C.

(2) Krokan, H. E., Standal, R., Slupphaug, G. (1997) *Biochem. J. 325*, 1–16.

(3) David, S. S., Williams, S. D. (1998) *Chem. Rev. 98*, 1221–1262.

(4) Blainey, P. C., van Oijen, A. M., Banerjee, A., Verdine, G. L., Xie, X. S. (2006) *Proc. Natl. Acad. Sci. U. S. A. 103*, 5752–5757.

(5) Roberts, R. J., Cheng, X. (1998) *Annu. Rev. Biochem. 67*, 181–198.

(6) Verdine, G. L., Bruner, S. D. (1997) *Chem. Biol. 4*, 329–334.

(7) Francis, A. W., David, S. S. (2003) *Biochemistry 42*, 801–810.

(8) Halford, S. E., Szczelkun, M. D. (2002) *Eur. Biophys. J. 31*, 257–267.

(9) Gowers, D. M., Halford, S. E. (2003) *EMBO J. 22*, 1410–1418.

(10) Gerland, U., Moroz, J. D., Hwa, T. (2002) *Proc. Natl. Acad. Sci. U. S. A. 99*, 12015–12020.

(11) Boon, E. M., Livingston, A. L., Chmiel, N. H., David, S. S., Barton, J. K. (2003) *Proc. Natl. Acad. Sci. U. S. A. 100*, 12543–12547.

(12) Boal, A. K., Yavin, E., Lukianova, O. A., O'Shea, V. L., David, S. S., Barton, J. K. (2005) *Biochemistry 44*, 8397–8407.

(13) Yavin, E., Boal, A. K., Stemp, E. D. A., Boon, E. M., Livingston, A. L., O'Shea, V. L., David, S. S., Barton, J. K. (2005) *Proc. Natl. Acad. Sci. U. S. A. 102*, 3546–3551.

(14) Yavin, E., Stemp, E. D. A., O'Shea, V. L., David, S. S., Barton, J. K. (2006) *Proc. Natl. Acad. Sci. U. S. A. 103,* 3610–3614.

(15) Kuo, C. F., McRee, D. E., Fisher, C. L., O'Handley, S. F., Cunningham, R. P., Tainer, J. A. (1992) *Science 258*, 434–440.

(16) Thayer, M. M., Ahern, H., Xing, D., Cunningham, R. P., Tainer, J. A. (1995) *EMBO J. 14*, 4108–4120.

(17) Fromme, J. C., Verdine, G. L. (2003) *EMBO J. 22*, 3461–3471.

(18) Fromme, J. C., Banerjee, A., Huang, S. J., Verdine, G. L. (2004) *Nature 427*, 652–656.

(19) Asahara, H., Wistort, P. M., Bank, J. F., Bakerian, R. H., Cunningham, R. P. (1989) *Biochemistry 28*, 4444–4449.

(20) Cunningham, R. P., Asahara, H., Bank, J. F., Scholes, C. P., Salerno, J. C., Surerus, K., Munck, E., McCracken, J., Peisach, J., Emptage, M. H. (1989) *Biochemistry 28*, 4450–4455.

(21) Fu, W., O'Handley, S., Cunningham, R. P., Johnson, M. K. (1992) *J. Biol. Chem. 267*, 16135–16137.

(22) O'Handley, S., Scholes, C. P., Cunningham, R. P. (1995) *Biochemistry 34*, 2528–2536.

(23) Xing, D., Dorr, R., Cunningham, R. P., Scholes, C. P. (1995) *Biochemistry 34*, 2537–2544.

(24) Porello, S. L., Cannon, M. J., David, S. S. (1998) *Biochemistry 37*, 6465–6475.

(25) Michaels, M. L., Pham, L., Nghiem, Y., Cruz, C., Miller, J. H. (1990) *Nucleic Acids Res. 18,* 3841–3845.

(26) Tsai–Wu, J. J., Liu, H. F., Lu, A. L. (1992) *Proc. Natl. Acad. Sci. U. S. A. 89,* 8779–8783.

(27) Lu, A. L., Tsai-Wu, J. J., Cillo, J. (1995) *J. Biol. Chem. 270,* 23582–23589.

(28) Bulychev, N. V., Varaprasad, C. V., Dorman, G., Miller, J. H., Eisenberg, M., Grollman, A. P., Johnson, F. (1996) *Biochemistry 35,* 13147–13156.

(29) Porello, S. L., Williams, S. D., Kuhn, H., Michaels, M. L., David, S. S. (1996) *J. Am. Chem.* Soc. *118,* 10684–10692.

(30) Porello, S. L., Cannon, M. J., David, S. S. (1998) *Biochemistry 37,* 6465–6475.

(31) Golinelli, M. P., Chmiel, N. H., David, S. S. (1999) *Biochemistry 38,* 6997–7007.

(32) Messick, T. E., Chmiel, N. H., Golinelli, M. P., Langer, M. R., Joshua-Tor, L., David, S.S. (2002) *Biochemistry 41,* 3931–3942.

(33) Drummond, T. G., Hill, M. G., Barton, J. K. (2003) *Nature Biotechnol. 21,* 1192–1199.

(34) Cowan, J. A., Lui, S. M. (1998) *Adv. Inorg. Chem. 45,* 313–350.

(35) Beinert, H. (2000) *J. Biol. Inorg. Chem. 5,* 2–18.

(36) Carter, C. W., Kraut, J., Freer, S. T., Alden, R. A., Sieker, L. C., Adman, E., Jensen, L. H. (1972) *Proc. Natl. Acad. Sci. U. S. A. 69,* 3526–3529.

(37) Gorodetsky, A. A., Barton, J. K. (2006) *Langmuir 22,* 7917–7922.

(38) Kelley, S. O., Barton, J. K., Jackson, N. M., Hill, M. G. (1997) *Bioconjugate Chem. 8,* 31–37.

(39) Kelley, S. O., Boon, E. M., Barton, J. K., Jackson, N. M., Hill, M. G. (1999) *Nucleic Acids Res. 27,* 4830–4837.

(40) Boon, E. M., Ceres, D. M., Drummond, T. G., Hill, M. G., Barton, J. K. (2000) *Nature Biotechnol. 18,* 1096–1100.

(41) Kelley, S. O., Barton, J. K., Jackson, N. M., McPherson, L. D., Potter, A. B., Spain, E. M., Allen, M. J., Hill, M. G. (1998) *Langmuir 14,* 6781–6784.

(42) Guo, L. H., Hill, H. A. O. (1991) *Adv. Inorg. Chem. 36,* 341–375.

(43) Armstrong, F. A. (1992) *Adv. Inorg. Chem. 38,* 117–163.

(44) Armstrong, F. A., Heering, H. A., Hirst, J. (1997) *Chem. Soc. Rev. 26,* 169–188.

(45) Camba, R., Armstrong, F. A. (2000) *Biochemistry 39,* 10587–10598.

(46) Armstrong, F. A., Wilson, G. S. (2000) *Electrochim. Acta 45,* 2623–2645.

(47) Nassar, A. F., Rusling, J. F., Nakashima, N. (1996) *J. Am. Chem. Soc. 118,* 3043–3044.

(48) Rusling, J. F. (1998) *Acc. Chem. Res. 31,* 363–369.

(49) Udit, A. K., Hill, M. G., Gray, H. B. (2006) *Langmuir 22,* 10854–10857.

(50) Boiteux, S.; O'Connor, T. R.; Laval, J. (1987) *EMBO J. 6,* 3177–3183.

(51) O'Connor, T. R. (1993) *Nucleic Acids Res. 21,* 5561–5569.

(52) Bowler, R., Davies, T. J., Hyde, M. E., Compton, R. G. (2005) *Anal. Chem. 77,* 1916–1919.

(53) Kim, Y., Long, E. C., Barton, J. K., Lieber, C. M. (1992) *Langmuir 8*, 496–500.

(54) Thomson, A. J., Breton, J., George, S. J., Butt, J. N., Armstrong, F. A., Hatchikian, E. C. (1991) *Biochem. Soc. Trans. 19*, 594–599.